FOSSIL BACTERIA IN CENOMANIAN–TURONIAN PHOSPHATE NODULES AND COPROLITES, BOHEMIAN CRETACEOUS BASIN, CZECH REPUBLIC

Khaldoun AL-BASSAM[1] & Patricie HALODOVÁ[2]

[1]*Czech Geological Survey, Klarov 3, 11821 Prague 1, Czech Republic;*
e-mail: albassam703@gmail.com
[2]*Czech Geological Survey, Geologicka 6, 15200 Prague 5, Czech Republic;*
e-mail: patricie.halodova@geology.cz

Abstract: Phosphatized biomorphs, resembling modern and ancient bacteria, were identified for the first time in phosphate nodules, present at the base of the Bílá Hora Formation (uppermost Cenomanian – lower Turonian), and in phosphate coprolites at the base of the Teplice Formation (upper Turonian) in the Bohemian Cretaceous Basin. They are present in colonies as filaments, coccoids, strings, rods and outgrowths, associated with the phosphate as part of the rock constituents and display the characteristics of fossilized bacteria. Two types of bacteria were identified: chemotrophic, sulphur-reducing bacteria in the phosphate nodules and phototrophic cyanobacteria in the phosphate coprolites. Microanalysis of some of the fossil bacteria revealed a fluoride-rich calcium phosphate composition, compatible with the composition of bulk samples, in which carbonate-fluorapatite is the main mineral in the phosphate nodules and coprolites. The environmental indications of these fossil bacteria support the interpretation of an anoxic environment of phosphogenesis in the latest Cenomanian – earliest Turonian and variable redox conditions of coprolite phosphatization in the late Turonian. The potential microbial role in phosphogenesis in the former may have involved the suboxic breakdown of P-rich organic matter by sulphur-reducing bacteria and the release of phosphorus in the pore water, leading to the biochemical precipitation of phosphate. The latter involved initial P-storage by phototrophic bacteria in an oxic environment, followed by P-release below the sediment–water interface under suboxic conditions and subsequent phosphatization of the coprolites.

Key words: Sulphur-reducing bacteria, cyanobacteria, phosphogenesis, apatite, Cretaceous.

Manuscript received 10 November 2017, accepted 3 September 2018

INTRODUCTION

Bacteria have been identified in many modern and ancient phosphogenic systems and were considered to facilitate phosphate mineralization and play a role in phosphogenesis (e.g., Gallardo, 1977; Soudry and Lewy, 1988; Reimers *et al.,* 1990; Nathan *et al.,* 1993; Lamboy, 1994; Schulz *et al.,* 1996; Schulz and Schulz, 2005; Berndmeyer *et al.,* 2012; Crosby and Bailey, 2012; Edwards *et al.,* 2012; Bailey *et al.,* 2013; Hiatt *et al.,* 2015).

It was demonstrated conclusively, using a radioactive tracer (^{33}P) and modern bacteria and sediments, that bacterially metabolized P led directly to apatite precipitation (Goldhammer *et al.,* 2010). Recent work indicates that the most efficient microbial processes to concentrate and promote the precipitation of apatite are bacterial sulphate reduction and bacterial sulphide oxidation (Arning *et al.,* 2009; Brock and Schulz-Vogt, 2011; Crosby and Bailey, 2012; Bailey *et al.,* 2013; Lepland *et al.,* 2013; Hiatt *et al.,* 2015). Although microbial mediation probably is essential for mobilizing

and redistributing phosphorus in surficial sediments, observations of both modern and ancient phosphogenic systems indicate the contributions of other factors in the formation of marine sedimentary phosphorites, including low sedimentation rates, strong bottom currents and an abundance of organic matter (Föllmi, 1996; Li and Schieber, 2015).

The importance of sulphur-reducing bacteria in the formation of modern marine phosphatic sediments has been demonstrated in numerous recent studies (e.g., Arning *et al.,* 2009; Berndmeyer *et al.,* 2012; Hiatt *et al.,* 2015). In sediments of marine upwelling systems, the degradation of organic matter *via* sulphate reduction is considered the predominant anaerobic oxidation process (Arning, 2008). The generally high P in pore water is believed to be due to the bacterial breakdown of organic matter and the concentration of polyphosphate largely by sulphur chemosynthetic bacteria (Schulz and Schulz, 2005; Arning *et al.,* 2009; Goldhammer *et al.,* 2010; Hiatt *et al.,* 2015).

Phototrophic sulphur-oxidizing bacteria, on the other hand, are abundant in modern and ancient marine phosphorite settings and are believed to play an important role in phosphogenesis. They are capable of storing phosphate under oxic conditions and releasing large amounts of dissolved orthophosphate into pore water under suboxic conditions, facilitating rapid apatite precipitation (Burnett, 1977; Reimers *et al.*, 1990; Schulz and Schulz, 2005; Goldhammer *et al.*, 2010; She *et al.*, 2014). The presence of sulphur-oxidizing bacteria in modern, oxygen-poor phosphogenic settings led many authors to interpret phosphatized filaments as fossilized sulphur bacteria and to propose that these organisms were involved in microbial-mediated phosphogenesis (Williams and Reimers, 1983; Reimers *et al.*, 1990; Nathan *et al.*, 1993; Krajewski *et al.*, 1994; Bailey *et al.*, 2009).

Various types of phosphate component have been recorded and described in several horizons of the Cenomanian and Turonian sequences of the Bohemian Cretaceous Basin. They are present in the form of nodules, internal bivalve moulds, sponges, intraclasts, crusts, shark teeth and coprolites (Žítt *et al.*, 1998, 2015; Wiese *et al.*, 2004; Čech *et al.*, 2005; Vodrážka *et al.*, 2009). The purpose of the present contribution is to report for the first time the presence of fossil bacteria in some of these phosphate components. The study focuses on the description, characterization and chemical composition of biomorphs <1–3 μm in size, believed to be fossil bacteria, in the phosphate nodules and phosphate coprolites of the Bílá Hora and Teplice formations, respectively. Their environmental implications and possible influence on phosphogenesis are discussed.

GEOLOGICAL SETTING

The Bohemian Cretaceous Basin (BCB) is an intracontinental basin, formed in the mid-Cretaceous as a seaway between the North Sea and the Tethys Ocean (Uličný, 1997, 2001). Its limits in the Czech Republic today extend from Brno in E Moravia across Bohemia to the N and W of Prague (Fig. 1). It is believed that the basin was formed by the reactivation of a fault system in the Variscan basement of the Bohemian Massif in the mid-Cretaceous (Uličný,
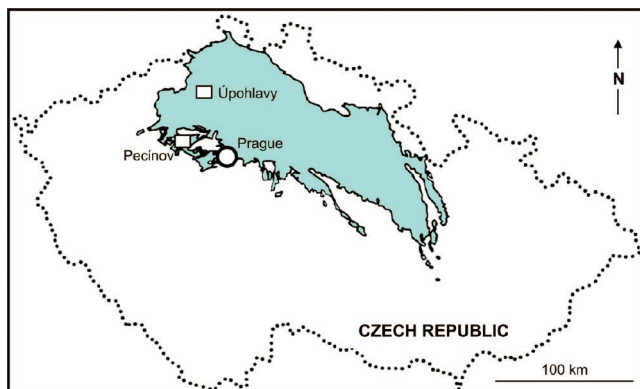
Fig. 1. Location map of the Bohemian Cretaceous Basin in the Czech Republic (after Wiese *et al.*, 2004), showing the sampling sites at the Pecínov and Úpohlavy quarries.

1997; Uličný *et al.*, 2009). Sedimentation within the BCB began during the late Albian or earliest Cenomanian (Valečka and Skoček, 1991), with displaced fault zones creating topographical lows adjacent to erosional source areas (Kear *et al.*, 2013).

The Cenomanian – lower Turonian sequence in the BCB is represented by the Peruc-Korycany Formation (Cenomanian) and Bílá Hora Formation (uppermost Cenomanian – –lower Turonian) (Čech *et al.*, 2005; Košťák *et al.*, 2018). The Peruc-Korycany Formation consists of three members: the Peruc and Korycany members (Čech *et al.*, 1980) and the Pecínov Member (Uličný, 1997). The Cenomanian––Turonian boundary in the BCB, as documented in the Pecínov Quarry section, is marked by stratigraphic condensation and erosional unconformity (Uličný *et al.*, 1997). On the basis of $\delta^{13}C$ analysis, the oceanic anoxic event (OAE 2), globally documented across this boundary, is reported to be missing in the Pecínov Quarry section, owing to erosion (Košťák *et al.*, 2018). The lithology of these rock units was reported by Čech *et al.* (1980) and Uličný (1997).

Peruc Member: The lower part comprises fining-upward cycles of grey sandstones and conglomerates, interbedded with grey mudstones. The upper part consists of grey sandstones and conglomerates, but is dominated by mudstones with root zones. Carbonaceous plant debris is common. The uppermost part consists of finely laminated, black mudstones with lenses and interbeds of siltstones and fine-grained sandstones.

Korycany Member: This consists of well sorted, fine- and medium-grained quartz sandstone and clayey sandstone. It contains thin, plant-rich layers and mud drapes and suffered intensive bioturbation. In the middle and upper parts of the section, a thin heterolithic facies is evident.

Pecínov Member: This is characterized by dark grey, clayey, variably calcareous, glauconitic, silty mudstone with brown, phosphatic nodules, pyrite, sponge spicules and a marine macrofauna (mostly bivalves and ammonites). The base of the member is marked by an erosional unconformity and a thin bed of pebbly sandstone. The late Cenomanian sequence at the Pecínov Quarry includes units P1–P4 of Uličný *et al.* (1997) (Fig. 2). They are separated by burrowed omission surfaces and consist of dark grey, glauconitic siltstone and mudstone with pyrite nodules and rare phosphate intraclasts; they are overlain by the Bílá Hora Formation at an omission surface (Košťák *et al.*, 2018).

Bílá Hora Formation: The lithology of the lowermost part of the Bílá Hora Formation at the Pecínov Quarry (Unit BH1 of Uličný *et al.*, 1997) is a dark grey, glauconitic mudstone with abundant brown and grey phosphate nodules. The contact with the underlying unit is marked by an erosion surface with dense *Chondrites* burrows (Fig. 2). The burrows pipe the sediments downwards into the underlying mudstone of the Pecínov Member.

The late Turonian sequence in the BCB is represented by the Jizera and Teplice formations. The lithology and biostratigraphy of the younger Teplice Formation were studied at the Úpohlavy Quarry by Čech *et al.* (1996) and Wiese *et al.* (2004), among others. This work deals with the phosphatic horizons in the lower part of the Teplice Formation.
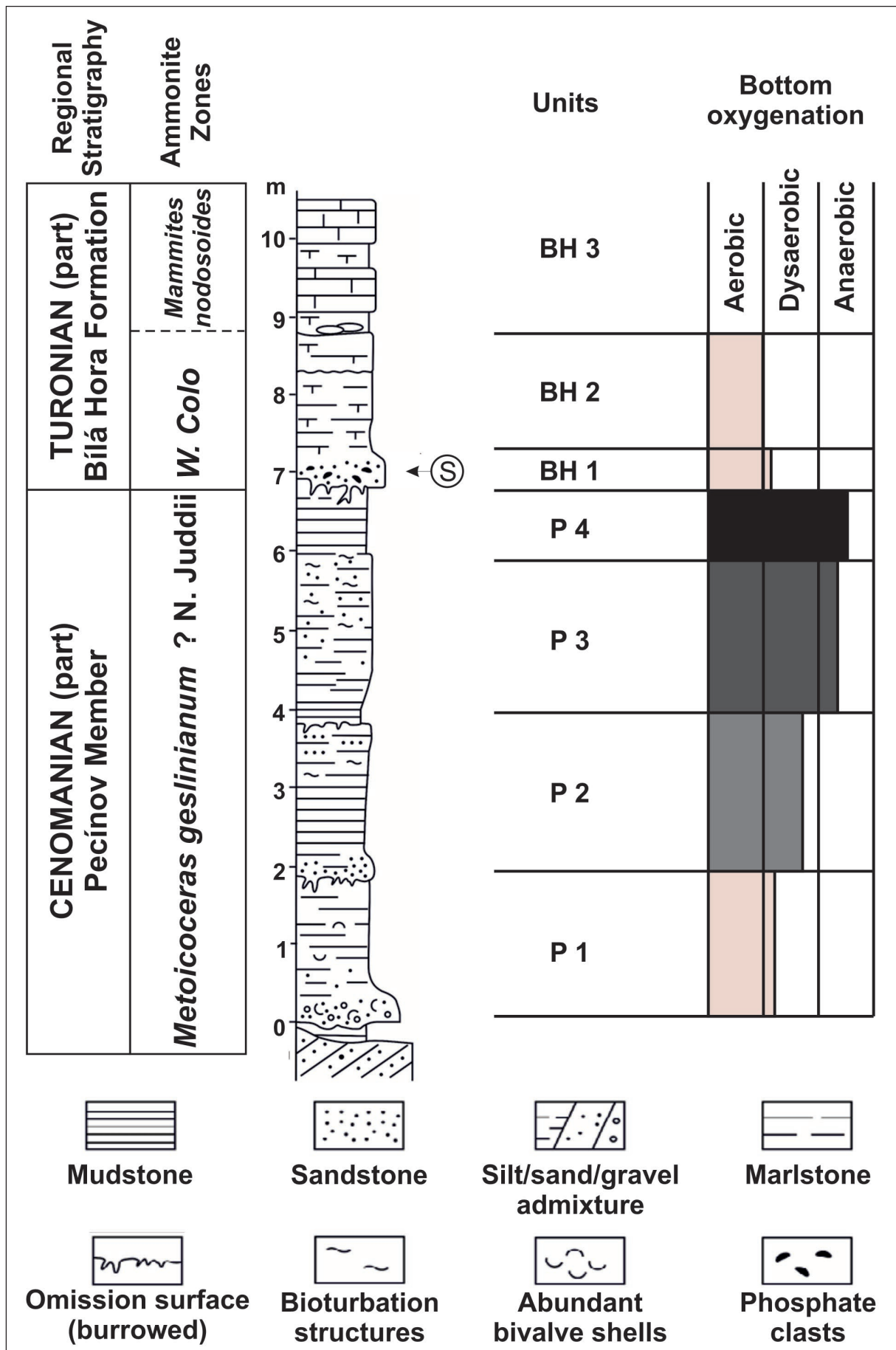
Fig. 2. Lithostratigraphic columnar section of the Cenomanian/Turonian boundary at the Pecínov Quarry (modified after Uličný *et al.,* 1997), showing lithological units, Ammonite Zones and bottom oxygenation. S – sampling location.

Teplice Formation: At the Úpohlavy Quarry, two phosphatic, coprolitic beds are recognized in the basal part of the Teplice Formation (Čech *et al.,* 1996). They are developed on highly bioturbated erosion surfaces and contain phosphate coprolites, phosphatic pebbles and phosphatized vertebrate remains. The boundary between the Jizera and Teplice formations is taken to be at the base of the Lower Coprolite Bed

(Fig. 3). It is 20–30 cm thick and glauconitic, with mm-size quartz grains and bored phosphate clasts. The contact is erosional, sharp and undulating, marked by skeletal debris and siliciclastic filling of burrows. The Lower Coprolite Bed grades upward into dark marl, which is terminated by another bioturbated and undulating erosional surface, sharply overlain by the Upper Coprolite Bed (Wiese *et al.,* 2004).
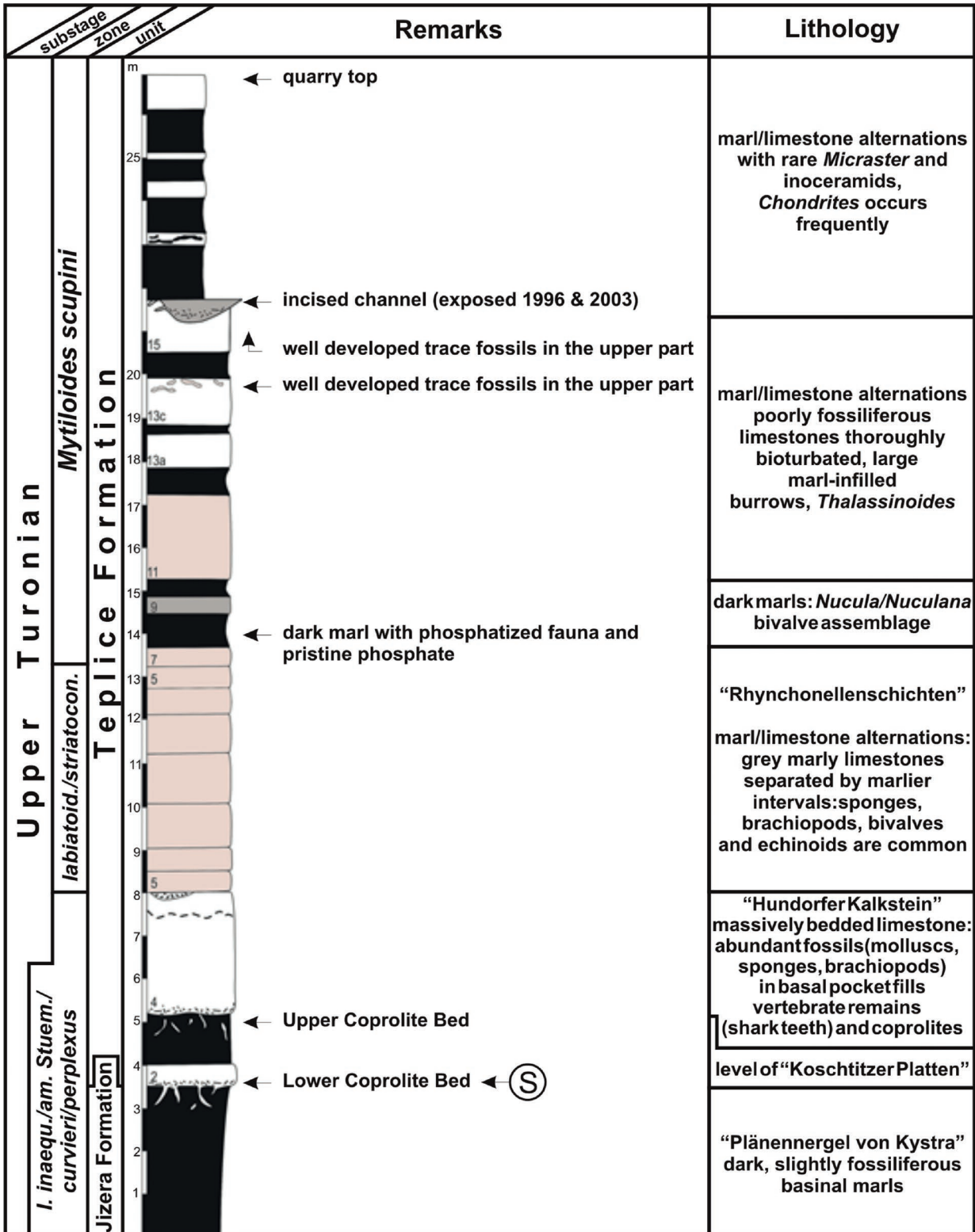

Fig 3. Lithostratigraphic columnar section of upper Turonian sequence at the Úpohlavy Quarry, showing location of coprolite beds at the base of the Teplice Formation (modified after Wiese *et al.,* 2004). S – sampling location.

MATERIAL AND METHODS

Several samples of phosphate nodules and phosphate co-prolites were extracted from the glauconitic, silty mudstone of the basal part of the Bílá Hora Formation (Unit BH1) at the Pecínov Quarry (Fig. 2) and from the Lower Coprolite Bed of the Teplice Formation at the Úpohlavy Quarry (Fig. 3) respectively. They were examined by means of a polarized-light optical microscope and their mineral phases were determined by X-ray diffractometry (XRD) at the Czech Geological Survey (CGS). The samples were crushed and homogenized in an agate mortar for the XRD analysis. The powder X-ray diffraction patterns of whole-rock samples were collected in Bragg-Brentano geometry on a Bruker D8 Advance Diffractometer, using Cu$K\alpha$ radiation and a Lynx Eye XE Detector. Automatic divergence slits (ADS 10 mm) and Soller slits 2.5° (in primary and secondary beam) were used. The data were collected in the angular range 4–80° 2θ with a 0.015° step and a time of 0.4 s. per step. The X-ray spectra were compared with standard XRD reflections for mineral identification (available in the software of the instrument). The chemical analysis of P_2O_5 in the phosphate nodules and coprolites studied was carried out following conventional wet chemistry procedures applied at the Czech Geological Survey (CGS) (Dempírová *et al.*, 2010) and the CO_3 content in the structure of the apatite was determined (as CO_2) from X-ray diffractograms, following the procedure of Gulbrandsen (1970).

For the detailed study of the samples, a scanning electron microscope (SEM) was used; the FEG–SEM Tescan MIRA 3GMU, fitted with a SDD X-Max 80mm² EDX detector (CGS laboratories), using Aztec Energy software for processing the spectra. The samples were coated prior to analysis with a 20-nm-thick layer of Au to avoid charging effects. The SEM imaging mode and the EDX analysis were conducted under conditions of 20 keV accelerating voltage, 1 nA probe current and WD 8 mm. The FEG–SEM has a primary electron beam focused to a very small probe of ~5 nm at given conditions, which allowed excellent spatial resolution for imaging. However, the excitation volume, from which X-rays are emitted, is much larger, typically 1–2 μm for this kind of matrix, so that the EDX spectrum can contain also the information about the surrounding material. To minimize possible matrix interference, some samples were reanalyzed without Au coatings, using a much lower energy of the incident electrons of 5 keV, focused to a very small probe of ~5 nm to reduce significantly the interaction volume of the analysed spot. For the estimation of this volume, the authors used Casino free software; the excited region for the matrix of the apatite composition modelled is in the range of 100–200 nm. To further reduce the interaction volume, the samples were tilted with respect to the electron beam (~60 deg.). The resulting EDX spectra have an interaction volume that is comparable to the size of the objects analysed and thus are representative of their chemical composition.

RESULTS

Petrographic description

Optical microscopy: The phosphate nodules of the Bílá Hora Formation are brown; and several centimetres in size, with polished surfaces and occasional borings. Under optical microscope examination, all phosphate nodules collected from the Bílá Hora Formation were seen to contain abundant grains of silt-size, angular quartz (<0.1 mm), glauconite pellets and organic residues, forming botryoidal or mammillary internal patterns (Fig. 4A, B). Some nodules show borings or cracks and cavities and most of them contain pyrite (Fig. 4C). The phosphate coprolites of the Teplice Formation are brown and cylindrical in shape, several centimetres long and about 1 cm in diameter, with convolutionary or coiled surfaces and pointed ends. They contain less foreign inclusions of quartz and glauconite, compared to the Bílá Hora phosphate nodules and are rich in organic residues, often showing biomorphic, tangled structures (Fig. 4D, E). Globular biomorphs, 0.02 mm in size, are common in the coprolites and some are hollow (Fig. 4F).

Scanning electron microscopy: SEM examination of phosphate nodule samples (Bílá Hora Formation) show well preserved, tubular and filamentous biomorphs, closely associated with the phosphate phase. They are less than 1 μm in diameter and may reach several μm in length, present as single items or as colonies of rods, filaments, bundles, strings and biofilms (Figs 5A–D, 6A, B, 7A, B). The phosphate matrix occasionally show well develped apatite crystallites (Fig. 5E) and framboidal pyrite (Fig. 5F). However, the apatite in the matrix is mostly present as crystallites of primitive shape (Fig. 8A) or as phosphate lumps without defnite crystal form (Fig. 8B). The SEM images of the phosphate coprolites show them as densely populated with colonies of simple, coccoidal biomorphs, 2–3 μm in diameter, with cell-wall structures and empty interiors (Figs 9A, B, 10).

Mineral and chemical characterization

Carbonate-fluorapatite is the major mineral in the phosphate nodules and coprolites studied, as shown in XRD analysis (Fig. 11A, B). It is crystalline with characteristic sharp XRD reflections, identical to spectra reported in the literature (e.g., Perdikatsis, 1991; Regnier *et al.,* 1994; Fig. 11C). The remaining accessory minerals, identified by means of optical microscopy and bulk-sample XRD analysis, are glauconite; quartz; pyrite and kaolinite. The P_2O_5 content of the phosphate components was found to range from 19.6 wt % to 26.5 wt. % in the phosphate nodules (8 samples) and from 22.8 wt. % to 28.4 wt. % in the coprolites (7 samples). The CO_3 content in the apatite structure, determined from the XRD spectra of five samples, ranges from 7.0 to 7.6 wt. % in the nodules and coprolites.

The chemical composition of the fossil biomorphs in the phosphate nodules was initially investigated by EDX microanalysis of Au-coated samples with a conventional accelerating voltage of 20 keV (Fig. 6A, B). The results obtained show P, Ca, Si, Al, Fe and C, in addition to Au (the coating material). To avoid interference from the surrounding ma-
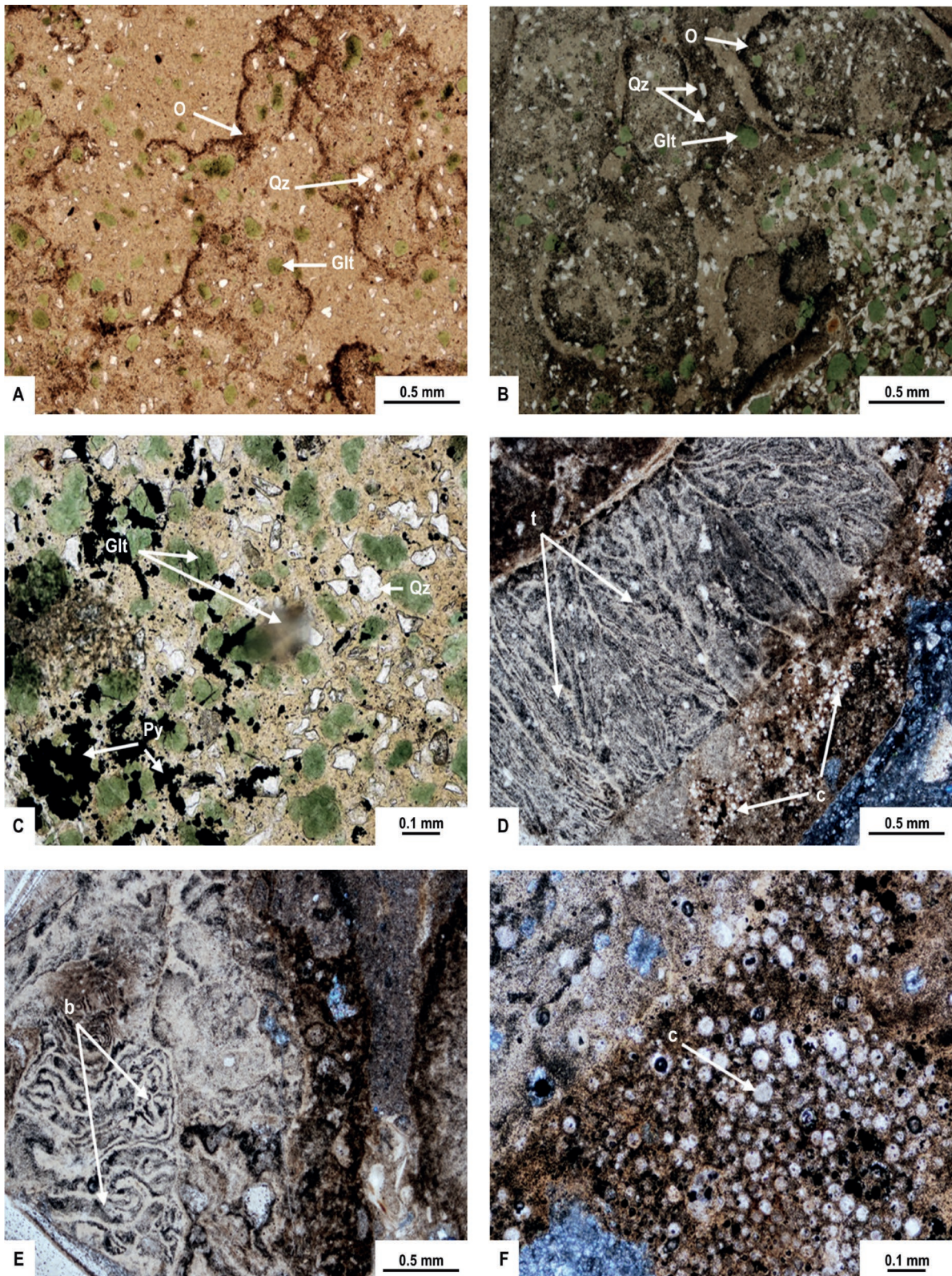
Fig. 4.   Polarized optical microscope photomicrographs. **A**. Phosphate nodule with quartz (Qz) and glauconite (Glt) inclusions in phosphate matrix rich in organic residues (o), Bílá Hora Formation, Pecínov Quarry (plain polarized light). **B**. Phosphate nodule is rich in organic residues (o) and contains inclusions of quartz (Qz) and glauconite (Glt), Bílá Hora Formation, Pecínov Quarry (plain polarized light). **C**. Phosphate nodule containing idiomorphic pyrite crystals (Py), angular quartz (Qz) and rounded glauconite pellets (Glt) in phosphate matrix, Bílá Hora Formation, Pecínov Quarry (plain polarized light). **D**. Phosphate coprolite showing phosphatized tangled structures (t) and coccoidal biomorphs (c), Teplice Formation, Úpohlavy Quarry, (semi-crossed nicols). **E**. Phosphate coprolite with organic (bacterial?) fabric (b) in phosphatized matrix, Teplice Formation, Úpohlavy Quarry (semi-crossed nicols). **F.** Phosphatized coccoidal biomorphs (c) in a phosphate coprolite, Teplice Formation, Úpohlavy Quarry (semi-crossed nicols). (Mineral abbreviations according to Whitney and Evans, 2010).
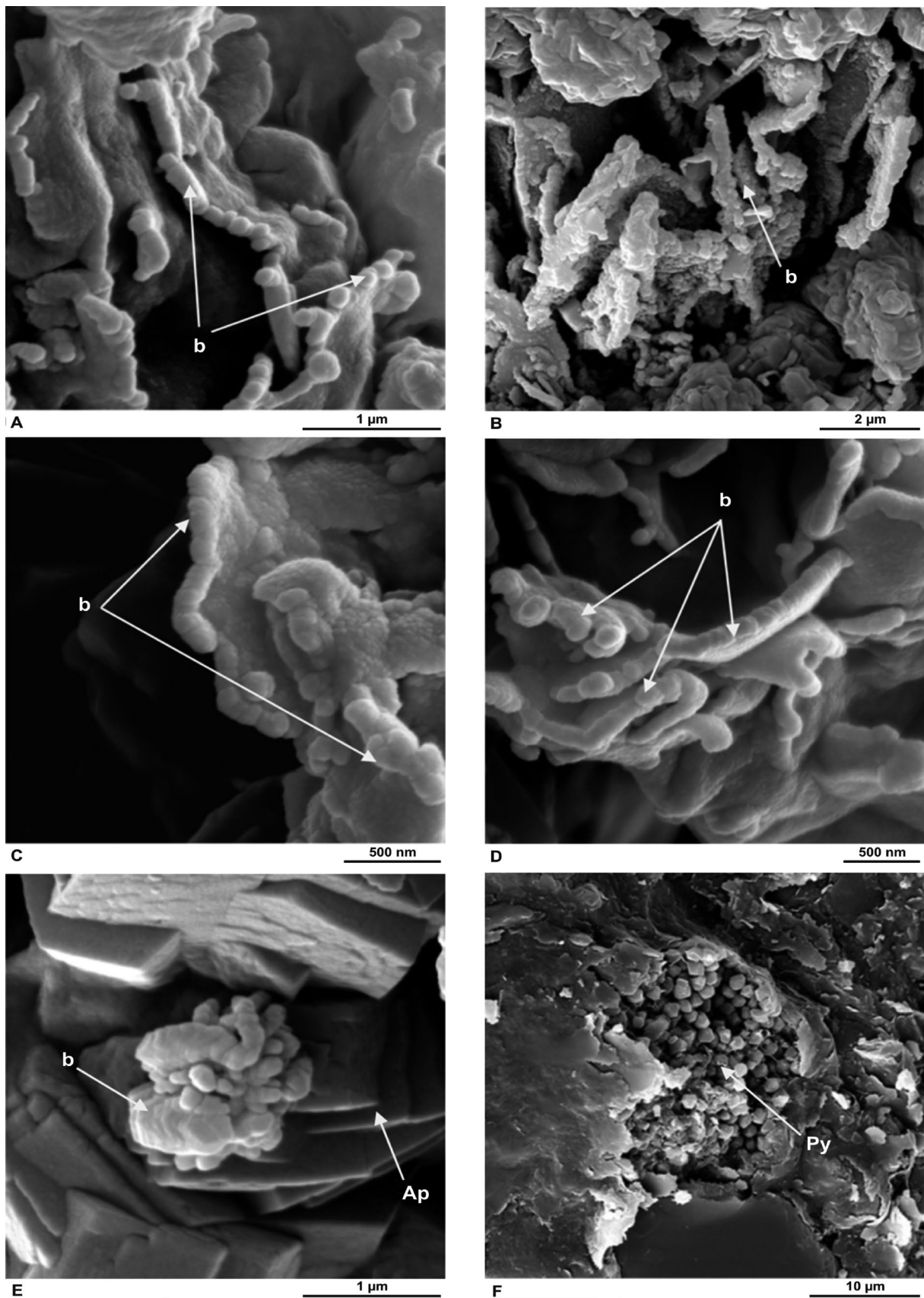
Fig. 5. Phosphatized bacterial biomorphs, apatite and framboidal pyrite in the phosphate nodules, Bílá Hora Formation, Pecínov Quarry. **A**. SEM image of bacterial strings, filaments and capsules (b) present as colonies in apatite matrix. **B**. SEM image of a bacterial colony (b). **C**. SEM image of a string of bacterial capsules (b) developed at the edge of phosphate biofilm. **D**. SEM image of phosphatized twisted filamentous bacteria (b) in apatite biofilm. **E.** SEM image of bacterial accumulation (b) on top of a stack of apatite crystals (Ap). **F.** SEM image of framboidal pyrite (Py) in a phosphate nodule.
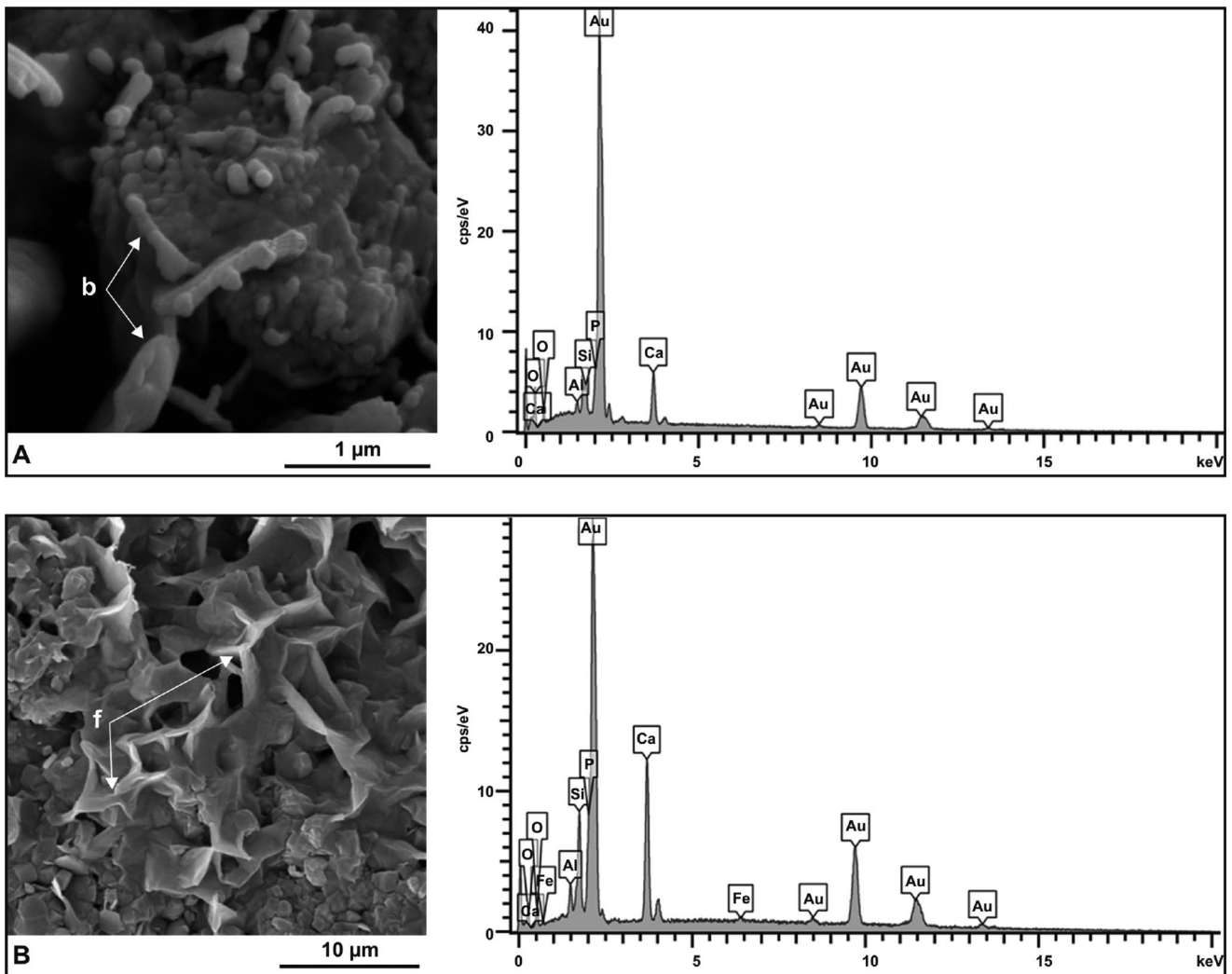
Fig. 6. SEM images and EDX spectra of Au-coated samples analysed using 20 keV beam energy. **A**. SEM image and spectrochemical analysis of bacteria-like filaments (b) with outgrowths and rod-shaped bacteria structures, showing rounded ends in a phosphate nodule, Bílá Hora Formation, Pecínov Quarry. **B.** SEM image and spectrochemical analysis of phosphatic biofilms (f) in a phosphate nodule, Bílá Hora Formation, Pecínov Quarry.

trix, uncoated nodules and coprolites samples were analysed with a low-energy beam of 5 keV and the excited region was reduced to 100–200 nm. The results obtained indicate a fluoride-rich calcium phosphate composition for these biomorphic nanostructures in the nodules (Fig. 7A, B), and the same for the coccoidal structures in the phosphate coprolites (Fig. 10). The EDX analysis of the phosphate matrix hosting these fossil biomorphs, under the same conditions of 5keV using uncoated samples, showed peaks of C, Si and Al of considerable intensity, in addition to the peaks of P, Ca and F (Fig. 8A, B).

DISCUSSION

Biogenic nature of the nanostructures

The nanostructures believed to be fossil biomorphs, identified in the SEM images of the phosphate nodules (Bílá Hora Formation) and phosphate coprolites (Teplice Formation), are of sizes and shapes, characteristic for recent and ancient bacteria (see Kazmierczak *et al.,* 1996; Astafieva and Rozanov, 2012; Bailey *et al*., 2013; Hiatt *et al.,* 2015). The nanofossils studied form integral parts of the textural constituents of the phosphate nodules in the Bílá Hora Formation and the phosphate coprolites in the Teplice Formation. They show cellular structures and colonial associations in cavities and appear as intrinsic parts of the rock constituents.

The fossil biomorphs in the phosphate nodules of the Bílá Hora Formation (Unit BH 1) have biological filaments, rods and cellular strings of microbial forms, characteristic for bacteria (Figs 5A–D, 7A, B). On the other hand, the biomorphs observed in the phosphate coprolites of the Teplice Formation (Lower Coprolite Bed) show simple, coccoidal forms with a mineralized, bacterial cell-wall structure (Figs 9A, B, 10). Most of the phosphate nodules examined in thin section contain black residues of organic origin (Fig. 4A, B). Resistant organic matter preserved in the apatite is considered to represent organic residues produced directly from bacteria, particularly bacterial cell-wall material, because of its refractory nature (Philp and Calvin, 1976;
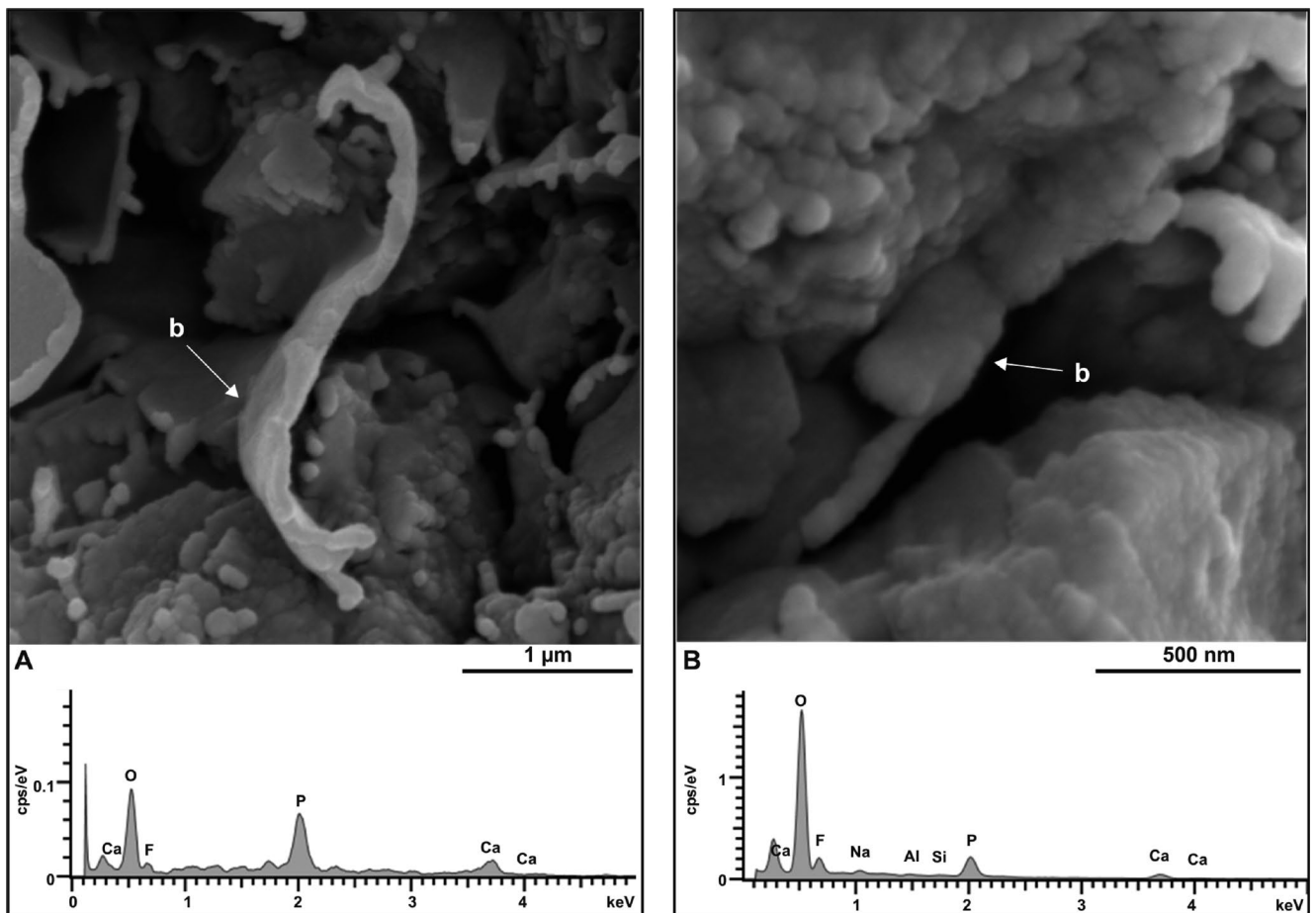
Fig. 7.   SEM images and EDX spectra of not coated samples analysed using low energy of the incident electrons of 5 keV. **A**. SEM image and spectrochemical analysis of twisted and branched bacterial filament (b) developed in a concentration of rod-shaped, bacteria-like outgrowths growing from apatite matrix, Bílá Hora Formation, Pecínov Quarry. **B**. SEM image and spectrochemical analysis of phosphatized string of bacteria capsules (b) in a colony of phosphatized bacteria outgrowths in a phosphate nodule, Bílá Hora Formation, Pecínov Quarry.

Kazmierczak *et al.,* 1996; Hiatt *et al.,* 2015). The above criteria, observed in this work, support the bacterial origin of the fossil biomorphs in the phosphate nodules and coprolites and are documented by many authors, who suggested a biogenic origin and the authenticity of such microstructures as fossil bacteria (Buick, 1990; Kazmierczak *et al.,* 1996; Westall, 1999; Schopf *et al.,* 2007).

Characterization of the fossil bacteria

Chemotrophic sulphur-reducing bacteria: The morphology of the filament and rod biomorphs observed in pores and cavities and along apatite margins in the phosphate nodules of the Bílá Hora Formation and their < 1 μm size (Figs 5–7) indicate that they are fossilized bacteria, comparable with their modern and ancient analogues. They resemble in shape, structure and size the sulphur-reducing bacteria noted in previously published images of ancient analogues (e.g., Bailey *et al.,* 2009; Astafieva and Rozanov, 2012; Hiatt *et al.* 2015). The filaments occur in bundles that curve and interweave and are incorporated in authigenic and early diagenetic apatite, but have no resemblance to the associated, inorganic structures of apatite. The present au-

thors suggest that these biomorphs are mineralized, formerly tubular structures and represent, in their opinion, on the basis of similarity to modern and ancient analogues, fossil sulphur-reducing bacteria that were preserved in the sediments by phosphatization. This identification is supported by the common presence of framboidal pyrite structures in the phosphate nodules (Fig. 5F), which is usually connected with vital activity of sulphur-reducing bacteria (Schieber, 1989; Hiatt *et al.,* 2015). Pyrite and other sulphide minerals can be produced simultaneously with apatite as a result of the activity of sulphate-reducing bacteria (Arning, 2008).

Phototrophic bacteria: The 2–3-μm-size, simple, coccoidal fossil biomorphs, present in the phosphate coprolites of the Lower Coprolite Bed of the Teplice Formation (Figs 9, 10), resemble benthic coccoidal cyanobacteria and are morphologically similar to ancient and modern analogues (see Kazmierczak *et al.,* 1996; Hoffman, 1999; Palinska *et al.,* 2006). Cyanobacteria have diverse morphological, biochemical and physiochemical properties (Palinska *et al*., 2006) and because of their relative structural complexity, the term "cyanobacteria" often has been used in a wide sense including all oxygenic photosynthetic prokaryotes (Hoffman, 1999). Fossil cyanobacteria are traditionally
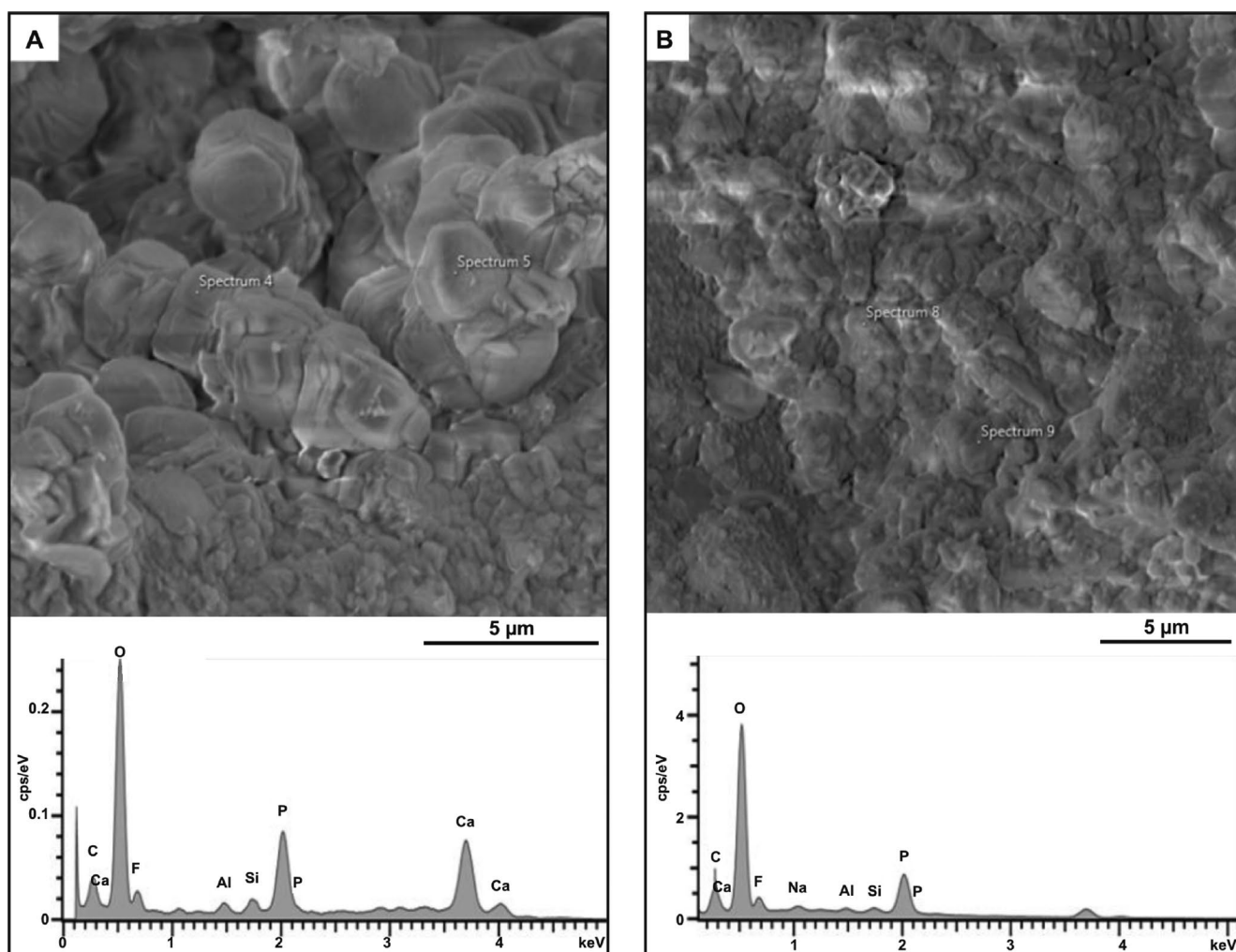
Fig. 8. SEM images and EDX spectra of not coated samples analysed using low energy of the incident electrons of 5 keV. **A.** SEM image and spectrochemical analysis of the matrix material in the phosphate nodule hosting bacteria in Fig. 7A, showing primitive apatite crystallites. **B.** SEM image and spectrochemical analysis of the matrix material in the phosphate nodule hosting bacteria in Fig. 7B, showing phosphate lumps.

characterized and identified by morphological properties, revealed by optical and scanning electron microscopy (Palinska *et al.*, 2006).

The coccoidal structures found in the phosphate coprolites cannot be mistaken for pollen or foraminifera or for inorganically precipitated calcium phosphate spherules or any other inorganic structures. This argument is based on their uniform size (2–3 μm in diameter), empty interior, cell morphology, the presence of a cell-wall structure (Fig. 9A, B) and their occurrence as colonies (Fig. 10). These colony-forming groups of capsules are more similar in size, shape and structure to coccoidal cyanobacteria than to any other type of bacteria (see Kazmierczak *et al.,* 1996; Hoffman, 1999; Palinska *et al.,* 2006; Astafieva and Rozanov, 2012). Cyanobacteria are unicellular and spherical; as well they perform oxygen-evolving photosynthesis to form coccoid cyanobacteria and cyanobacterial capsules (see Kazmierczak *et al.,* 1996; Vincent, 2009). The presence of fossil cyanobacteria in colonies in the phosphate coprolites, forming an integral part of the phosphate phase, indicates the flourishing of these microbes during early diage-

netic processes. Their growth was enhanced by the warm mid-Cretaceous climate, the availability of light in a shallow-marine environment and by using phosphorus, nitrogen and other nutrients, expected to be present in the faecal material of the predator from considerations of its type of diet (see Fig. 9B).

Mineralogy and chemical composition

The P_2O_5 contents of the phosphate nodules (22.8––28.4 wt. %) and coprolites (19.6–26.5 wt. %) correspond to carbonate-fluorapatite content of 63–85 modal % in the former and 72–90 modal % in the latter, considering that carbonate-fluorapatite contains about 34 wt.% P_2O_5. The CO_3 content in the apatite structure, determined from the XRD spectra of the apatite in the nodules and coprolites, ranging from 7.0 to 7.6 wt. %, confirm the carbonate-fluorapatite composition in the phosphate components studied, found by XRD analysis (Fig. 11A, B). However, it was a challenge to obtain a reliable EDX chemical analysis of the minute (<1–3 μm) structures with minimum interference from the
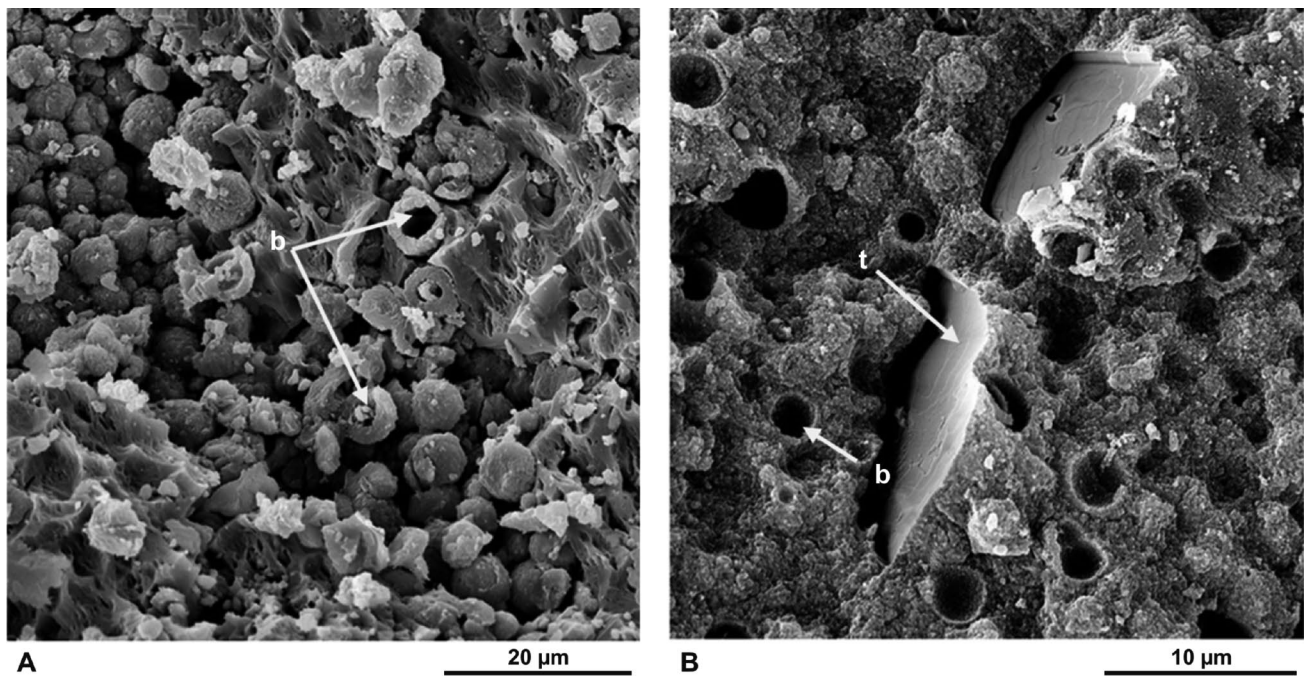
Fig. 9. SEM images of (**A**) a colony of spherical biomorphs with an empty interior (b) resembling cyanobacteria, developed in the phosphatized biofilms of a phosphate coprolite, Teplice Formation, Úpohlavy Quarry, and (**B**) phosphatized spherical bacterial cells (b) showing well-defined cell walls closely associated with a phosphatic fish tooth (f) in a phosphate coprolite, Teplice Formation, Úpohlavy Quarry.

matrix. Most micro-analytical techniques, including EPMA and micro-XRD, would face problems from various degrees of interference in attempts to analyse such micron-size structures. They may provide adequate spatial resolution, but certainly cannot avoid interference from the matrix.

This problem was faced, when using conventional beam energy of 20 keV in the EDX microanalysis of Au-coated nodule samples, which showed in addition to P and Ca, peaks of Si and Al with considerable intensities (Fig. 6A, B). These could have been produced from the minor amounts of quartz and aluminosilicates present in the matrix. The traces of Fe peaks in these EDX spectra (Fig. 6B) may be due to pyrite that is commonly present in the nodules, whereas the traces of carbon (Fig. 6A, B) may be attributed to more than one source. It may attest to the biological nature of these nanostructures, or to the organic residues present in the phosphate matrix and/or it may represent structural CO_3 of the carbonate-fluorapatite. These suggestions infer that the P and Ca peaks, detected in the Au-coated samples hosting the bacterial structures, could have been enhanced by the apatite and other minor mineral constituents present in the matrix, when using conventional voltage of 20 keV. Thus, these results are probably not conclusive enough to determine the composition of the bacteria structures.

To remove possible matrix interference with the chemical composition of the bacterial structures, the EDX microanalysis was performed using uncoated samples of nodules and coprolites, under a low-energy beam current of 5 keV and electron beam focused to a very small probe of ~5 nm, where the excited region was reduced to 100–200 nm. The results point to a fluoride-rich calcium phosphate as the ma-
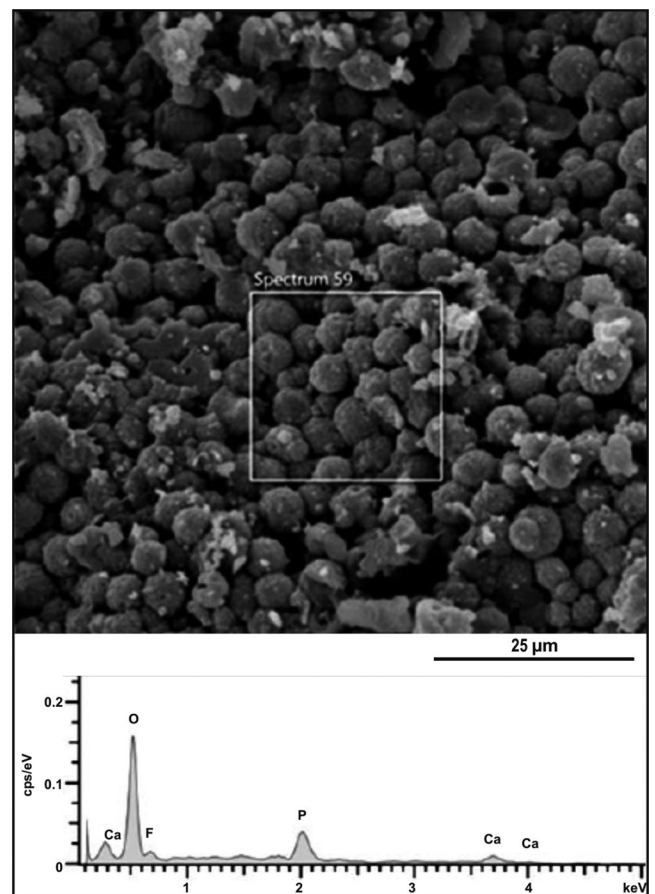

Fig. 10. SEM image (**A**) and spectrochemical analysis (**B**) of a colony of spherical phosphatized biomorphs with uniform size in a phosphate coprolite, Teplice Formation, Úpohlavy Quarry. Uncoated sample analysed using low energy of the incident electrons of 5 keV..
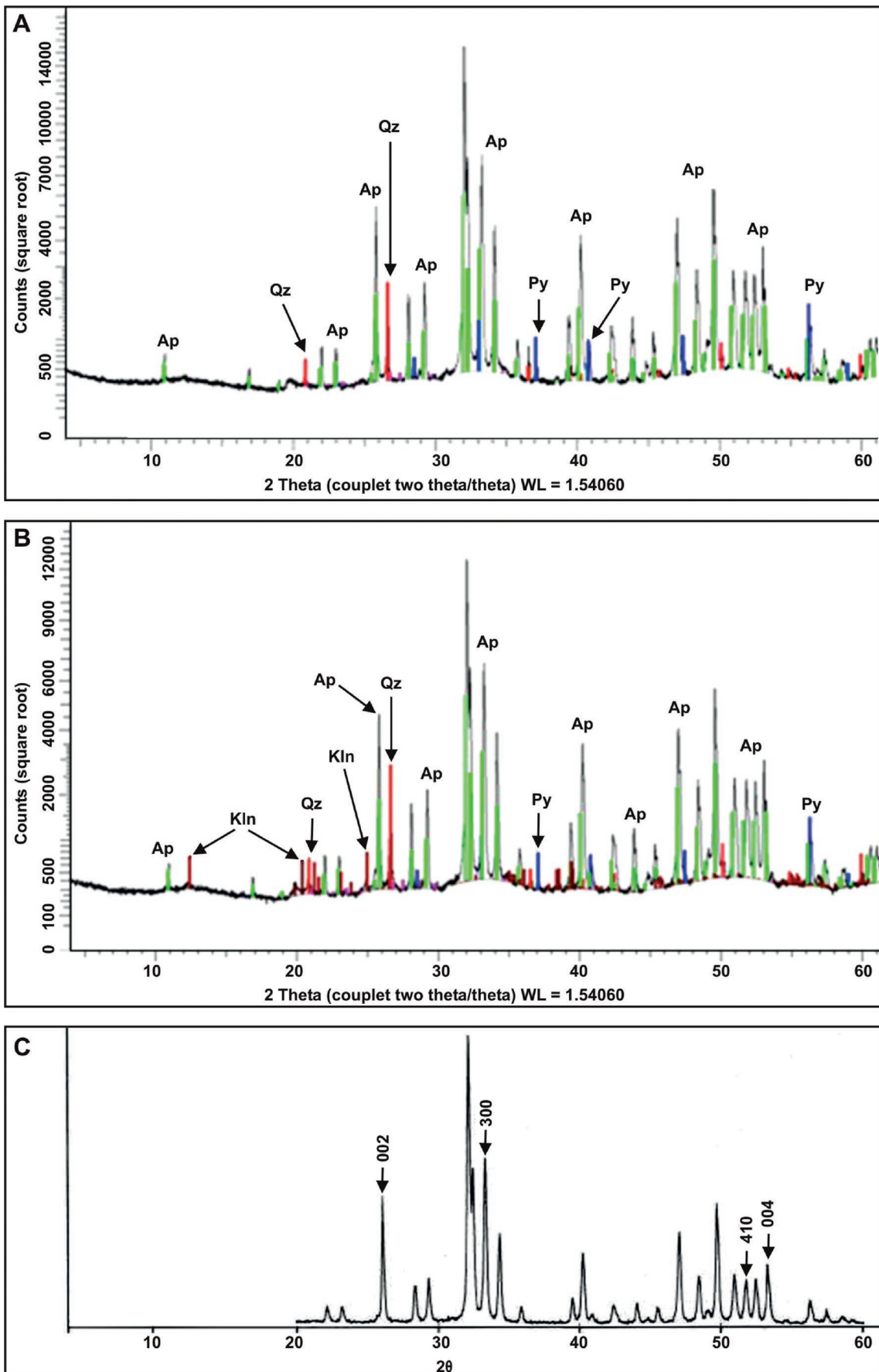
Fig. 11. X-ray diffractograms of a phosphate nodule **(A)** and phosphate coprolite **(B)** showing carbonate–fluorapatite spectra (Ap) as the major phase (green) with traces of quartz (Qz) (red), pyrite (Py) (blue) and kaolinite (Kln) (brown). **C.** Typical X–ray diffraction spectra of carbonate–fluorapatite (Regnier *et al.,* 1994).

jor composition with Al and Si impurities absent or occurring only as trace amounts (Figs 7A, B, 10). Carbon was not detected in these spectra possibly because of the low concentration and low energy of the beam current applied.

The EDX analysis of the matrix hosting the fossil bacteria structures in the uncoated nodules samples under the same conditions show peaks of P, Ca, and F, corresponding to the apatite composition of the matrix. They also show peaks of Si and Al of considerable intensity (Fig. 8A, B) corresponding to inclusions of quartz and aluminosilicates present in the matrix. Carbon was also detected in the matrix spectra, corresponding to organic matter and structural CO_3 of the apatite. These results indicate that the special conditions adopted in the analysis of these <1–3 μm biostructure have sufficiently reduced the interference from the matrix, evidenced by the diminishing peaks of Si and Al in the spectra of the fossil bacteria, compared to those in the matrix under the same analytical conditions. The peaks of Al and Si would have appeared in the bacteria spectra, if there had been matrix interference. The results, showing Ca, P and F peaks only, are relatively close to the composition of carbonate-fluorapatite that dominates the mineralogy of the nodules and coprolites; they conform to the mineral composition of bulk samples, determined by XRD analysis, indicating that these fossil bacteria are phosphatized.

Environmental implications

The type and habitat of the fossil bacteria, recognized in the phosphate components studied, may be useful in characterizing environmental conditions during their depositional history. The presence of chemotrophic sulphur-reducing bacteria in the phosphate nodules indicates anoxic conditions during the latest Cenomanian in the Pecínov Quarry section, which is compatible with the globally recognized oceanic anoxic event (OAE2), detected across the Cenomanian–Turonian boundary (e.g., Uličný *et al.,* 1997; Jarvis *et al.,* 2006; Košťák *et al.,* 2018). The pristine phosphate deposits, however, were reworked and matured in the shallowing event that followed and were mechanically emplaced in the overlying lowest lower Turonian units (Laurin, 1996 and according to the field observations of the present authors), but they still hold the bacterial signature of the latest late Cenomanian oceanic anoxia. The signature of this anoxic event was also shown in the REE patterns of distribution in these phosphate nodules (Al-Bassam and Magna, 2018). Borings, often observed in the phosphate nodules, are younger trace fossils and indications of the oxic conditions that prevailed during the shallowing event and subsequent reworking of the phosphate components.

Cyanobacteria, on the other hand, are phototrophic bacteria that can thrive in various aquatic environments, including marine and fresh water as well as in soil. They occur over a wide range of water temperature, pH, redox potential and salinity, hence they are not of great value as palaeoenvironmental indicators for ancient sedimentary systems. However, cyanobacteria are reported to prefer warm temperatures for growth (>15ºC) and alkaline conditions and can tolerate water salinities of up to 30 gm/l (Vincent, 2009). They usually thrive in oxygenated environments, but some types of

cyanobacterial are characteristic components of sediments in the oxygen minimum zones of modern oceans (Fossing *et al*., 1995; Buck and Barry, 1998; Schulz *et al.,* 1999; Gallardo and Espinoza, 2007). In the present study, the authors suggest two successive environments for these bacteria; an earlier one, where they thrived in the faecal material and stored phosphorus in the shallow, marine environment and warm, oxic conditions of the photic zone, and a later stage, in which they were buried below the sediment–water interface, where they released phosphorus under suboxic conditions.

Potential role of bacteria in phosphogenesis

Phosphate nodules: The close association of the sulphur-reducing fossil bacteria with the apatite phase, shown in the SEM images, indicates that they may have mediated in phosphate precipitation in the manner described and documented in recent phosphogenic environments (e.g., Bailey *et al.,* 2013). The bacterial mediation in phosphogenesis also has been shown by various authors to lead to apatite precipitation and the potential encapsulation of the bacteria in modern and ancient phosphogenic environments (Soudry and Champetier 1983; Krajewski *et al.,* 1994; Schulz *et al.,* 1999; Schulz and Schulz, 2005; Konhauser, 2007; Arning *et al.,* 2009; Hiatt *et al.,* 2015).

The main source of phosphorus in the late Cenomanian phosphogenic event(s) in the BCB was most probably organic matter, entrapped in the sediments, which reportedly contain up to a few weight percent P that is very efficiently returned to seawater under anoxic conditions (Froelich *et al*., 1982; Ingall and Jahnke, 1994). The authors suggest that the potential role of the chemotrophic sulphur-reducing bacteria in phosphogenesis was to break down sedimentary organic matter and to release phosphate in the suboxic marine environment below the sediment–water interface. In such an environment, sulphur-reducing bacteria can also liberate phosphate, sorbed onto Fe-oxide and Fe-oxyhydroxide particles, and concentrate polyphosphate compounds inside their cells. When orthophosphate is available in pore waters, some bacteria can influence phosphogenesis with the precipitation of authigenic phosphate minerals, which can cause self-phosphatization, where the cells become embedded in the phosphate matrix, preserving detailed intracellular structures (Benzerara *et al.,* 2004; Raff *et al.,* 2008; She *et al.,* 2014). Phosphatic precursors to apatite are thought to commonly nucleate on bacterial cells, which leads to the phosphatization of the microbes (Bailey *et al.,* 2007). The record of the biomineralization and microbial mediation in phosphogenesis of the phosphate nodules at the base of the Bílá Hora Formation is well preserved in the phosphatized fossil bacteria.

Phosphate coprolites: The phosphate coprolites in the upper Turonian Teplice Formation represent another phosphogenic event in the sequence of the BCB studied. The coprolites witnessed several stages of diagenetic phosphatization in the marine environment, with possible mediation by phototrophic bacteria. Cyanobacteria flourished, while the coprolites were lying on the shallow sea floor within the photic zone, storing the phosphorus that was available in the unconsolidated faecal material. The authors

suggest that the role of these bacteria in phosphogenesis was manifested later, following burial below the sediment––water interface, and included the supply of phosphorus to the interstitial pore water in suboxic conditions. At this position, the phosphorus stored in the cyanobacteria cells could have been released. Cyanobacteria are known to store phosphorus as part of their metabolism and this can be released back to the interstitial environment under suboxic conditions (Schulz and Schulz, 2005; Goldhammer *et al*., 2010; Brock and Schulz-Vogt, 2011). The concluding stages took place below the sediment–water interface under less oxygenated conditions and witnessed phosphorus accumulation and precipitation as calcium phosphate, gradually replacing the original coprolite constituents. The intimate presence of phosphatized cyanobacteria in the phosphate coprolites supports their association with the phosphatization process, possibly by serving as nuclei for the early phosphate precipitates. The subsequent crystallization of apatite in the coprolites was most probably accomplished through long periods of residence time and contact with P-rich seawater or pore water.

Inorganic phosphogenesis

Other mechanisms of phosphate precipitation cannot be excluded and may have contributed to the phosphogenic events of the upper Cenomanian – lower Turonian and upper Turonian in the BCB. Inorganic chemical precipitation of phosphate could have been one of these mechanisms, demonstrated by the diagenetic crystallization of the phosphate and the development of the apatite crystallites that were observed in some SEM images (Figs 5E, 8A). The development of apatite crystallites cannot be attributed to a bacterial role; it indicates a digenetic process of inorganic crystal growth of apatite on the original phosphate precipitates. Moreover, the inorganic phosphatization of carbonate precursors, such as bivalve moulds, sponges and bioclasts, could have been another mode of phosphogenesis in the Cenomanian–Turonian sequence of the BCB, evidenced by the common presence of these phosphatized components in various horizons of the sequence (e.g., Žítt *et al.,* 1998; Wiese *et al.,* 2004; Vodrážka *et al.,* 2009; Žítt *et al.,* 2015).

CONCLUSIONS

Two types of bacteria were recognized in this study, closely associated with carbonate-fluorapatite in phosphate nodules (Bílá Hora Formation) and phosphate coprolites (Teplice Formation). The microbial fossils, identified in the phosphate nodules as < 1-μm-size filaments, strings of cells and rods, resemble chemotrophic, sulphur-reducing bacteria. On the other hand, the larger (2–3 μm), coccoidal biomorphs, with well-defined cell walls and empty interiors, identified in the phosphate coprolites, are most probably some kind of phototrophic cyanobacteria. These biomorphs are phosphatized and composed of fluoride-rich calcium phosphate.

The presence of chemotrophic, sulphur-reducing bacteria in the phosphate nodules indicates anoxic conditions during the latest Cenomanian in the Pecínov Quarry section, which is compatible with the globally recognized anoxic conditions across the Cenomanian–Turonian boundary. On the other hand, the authors suggest two successive environments for the phosphatization of the upper Turonian phosphate coprolites. In an earlier one, the cyanobacteria thrived and stored phosphorus in the faecal material in shallow, warm and oxic conditions of the marine photic zone. In a later stage, the coprolites were buried below the sediment–water interface under suboxic conditions, where cyanobacteria released phosphorus in the interstitial environment.

The role of sulphur-reducing bacteria in the phosphate nodules may have included the breakdown of P-rich, organic matter and the authigenic, biochemical precipitation of phosphate in anoxic conditions below the sediment-water interface. On the other hand, the phototrophic cyanobacteria stored the phosphorus contained in the organic matter of the coprolites under oxic conditions, followed by the subsequent release of phosphate under suboxic conditions, leading to gradual phosphatization of the coprolites together with the bacterial biomorphs as fossil bacteria.

REFERENCES

Al-Bassam, K. & Magna, T., 2018. Distribution and significance of rare earth elements in Cenomanian–Turonian phosphate components and mudstones from the Bohemian Cretaceous Basin, Czech Republic. *Bulletin of Geosciences,* 93: 347–368.

Arning, E. T., 2008. *Phosphogenesis in Coastal Upwelling Systems-Bacterially-Induced Phosphorite Formation.* Ph.D. thesis, University of Bremen, Germany, 149 pp.

Arning, E. T., Birgel, D, Brunner, B. & Peckmann, J., 2009. Bacterial formation of phosphatic laminites off Peru. *Geobiology,* 7: 295–307.

Astafieva, M. M. & Rozanov, A. Yu., 2012. Bacterial-paleontological study of Early Precambrian weathering crusts. *Earth Science Research,* 1: 163–170.

Bailey, J. V., Corsetti, F. A., Greene, S. E., Crosby, C. H., Liu, P. & Orphan, V. J., 2013. Filamentous sulfur bacteria preserved in modern and ancient phosphatic sediments: implications for the role of oxygen and bacteria in phosphogenesis. *Geobiology,* 11: 397–405.

Bailey, J. V., Joye, S. B., Kalanetra, K. M., Flood, B. E. & Corsetti, F. A., 2007. Evidence of giant sulfur bacteria in Neoproterozoic phosphorites. *Nature,* 445: 198–201.

Bailey, J. V., Orphan, V. J., Joye, S. B. & Corsetti, F. A., 2009. Chemotrophic microbial mats and their potential for preservation in the rock record. *Astrobiology,* 9: 843–859.

Benzerara, K., Yoon, T. H., Tyliszczak, T. Constantz, B., Spormann, A. M. & Brown, G. E., 2004. Scanning transmission X-ray microscopy study of microbial calcification. *Geobiology,* 2: 249–259.

Berndmeyer, C., Birgel, D., Brunner, B., Wehrmann, L. M., Jons, N., Bach, W., Arning, E. T., Föllmi, K. B. & Peckmann, J., 2012. The influence of bacterial activity on phosphorite formation in the Miocene Monterey Formation, California. *Palaeogeography, Palaeoclimatology, Palaeoecology,* 317–318: 171–181.

Brock, J. & Schulz-Vogt, H. N., 2011. Sulfide induces phosphate release from polyphosphate in cultures of a marine Beggiatoa strain. *International Society for Microbial Ecology (ISME) Journal,* 5: 497–506.

Buck, K. R. & Barry, J. P., 1998. Monterey Bay cold seep fauna: quantitative comparison of bacterial mat meiofauna with non-seep control sites. *Cahiers de Biologie Marine,* 39: 333–335.

Buick, R., 1990. Microfossil recognition in Archean rocks: an appraisal of spheroids and filaments from a 3500 M.Y. old chert-barite unit at North Pole, Western Australia. *Palaios,* 5: 441–459.

Burnett, W. C., 1977. Geochemistry and origin of phosphorite deposits from off Peru and Chile. *Geological Society of America Bulletin,* 88: 813–823.

Čech, S., Klein, V., Kříž, J. & Valečka, J., 1980. Revision of the Upper Cretaceous stratigraphy of the Bohemian Cretaceous Basin. *Věstnik Ústředniho Ústavu Geologického,* 55: 277–296.

Čech, S., Hradecká, L., Laurin, J., Štaffen, Z., Švábenická, I. & Uličný, D., 1996. Úpohlavy quarry: record of the late Turonian sea-level oscillations and synsedimentary tectonic activity. Stratigraphy and Facies of the Bohemian-Saxonian Cretaceous Basin. In*: Field Trip Guide, 5th International Cretaceous Symposium, Freiberg*, pp. 32–42.

Čech, S., Hradecká, L., Svobodová, M. & Švábenická, L., 2005. Cenomanian and Cenomanian-Turonian boundary in the southern part of the Bohemian Cretaceous Basin, Czech Republic. *Bulletin of Geosciences,* 80: 321–354.

Crosby, C. H. & Bailey, J. V., 2012. The role of microbes in the formation of modern and ancient phosphatic mineral deposits. *Frontiers in Microbiology,* 3: 1–7.

Dempírová, L., Šikl J., Kašičková, R., Zoulková, V. & Kříbek, B., 2010. The evaluation of precision and relative error of the main components of silicate analyses in Central Laboratory of the Czech Geological Survey. Geoscience Research Reports, 43: 326–330

Edwards, C. T., Pufahl, P. K., Hiatt, E. E. & Kyser, T. K., 2012. Paleoenvironmental and taphonomic controls on the occurrence of paleoproterozoic microbial communities in the 1.88 Ga Ferriman Group, Labrador Trough. Canada. *Precambrian Research,* 212–213: 91–106.

Föllmi, K. B., 1996. The phosphorus cycle, phosphogenesis and marine phosphate-rich deposits. *Earth Science Review,* 40: 55–124.

Fossing, H., Gallardo, V. A., Jorgensen, B. B., Huttel, M., Nielsen, L. P., Schulz, D., Canfield, E., Forster, S., Glud, R. N., Gundersen, J. K., Kuver, J., Ramsing, N. B., Teske, A., Thamdrup, B. & Ulloa, O. 1995. Concentration and transport of nitrate by the mat-forming sulfur bacterium *Thioploca. Nature,* 374: 713–715.

Froelich, P. N., Bender, M. L., Luedtke, N. A., Heath, G. R. & Devries, T., 1982. The marine phosphorus cycle. *American Journal of Science,* 282: 474–511.

Gallardo, V. A., 1977. Large benthic microbial communities in sulfide biota under Peru-Chile subsurface counter current. *Nature,* 268: 331–332.

Gallardo, V. A. & Espinoza, C., 2007. New communities of large filamentous sulfur bacteria in the eastern South Pacific. *International Microbiology,* 10: 97–102.

Goldhammer, T., Bruchert, V., Ferdelman, T. G. & Zabel, M., 2010. Microbial sequestration of phosphorus in anoxic upwelling sediments. *Nature Geoscience,* 3: 557–561.

Gulbrandsen, R. A., 1970. Relation of carbon dioxide content of apatite of the Phosphoria Formation to regional facies. *U.S. Geological Survey Professional Paper, 700B*: B9–B13.

Hiatt, E. E., Pufahl, P. K. & Edwards, C. T., 2015. Sedimentary phosphate and associated fossil bacteria in a Paleoproterozoic tidal flat in the 1.85 Ga Michigamme Formation, Michigan, USA. *Sedimentary Geology,* 319: 24–39.

Hoffman, L., 1999. Marine cyanobacteria in tropical regions: diversity and ecology. *European Journal of Phycology*, 34: 371–379.

Ingall, E. & Jahnke, R., 1994. Evidence for enhanced phosphorus regeneration from marine sediments overlain by oxygen depleted waters. *Geochimica et Cosmochimica Acta,* 58: 2571–2575.

Jarvis, I., Gale, A. S., Jenkyns, H. C. & Pearce, M. A., 2006. Secular variation in Late Cretaceous carbon isotopes: a new δ^{13}C carbonate reference curve for the Cenomanian–Campanian (99.6–70.6 Ma). *Geological Magazine*, 143: 561– 608.

Kazmierczak, J. Coleman, M. L., Gruszczynski, M. & Kempe, S., 1996. Cyanobacterial key to the genesis of micritic and peloidal limestones in ancient seas. *Palaeontologica Polonica,* 41: 319–338.

Kear, B. P., Ekrt, B., Prokop, J. & Georgalis, G., 2013. Turonian marine amniotes from the Bohemian Cretaceous Basin, Czech Republic. *Geological Magazine*, 151: 183–198.

Konhauser, K. O., 2007. *Introduction to Geomicrobiology*. Blackwell Science, London, 425 pp.

Košťák, M., Čech, S., Uličný, D., Sklenář, J., Ekrt, B. & Mazuch, M., 2018. Ammonites, inoceramids, and stable carbon isotopes of the Cenomanian–OAE2 interval in Central Europe: Pecínov quarry, Bohemian Cretaceous Basin (Czech Republic). *Cretaceous Research*, 87: 150–173.

Krajewski, K. P., van Cappellen, P., Trichet, J., Kuhn, O., Lukas, J., Martin-Algarra, A., Prevot, L., Tewari, V. C., Gasper, I., Knight, R. I. & Lamboy, M., 1994. Biological processes and apatite formation in sedimentary environments. *Eclogae Geologicae Helvetica*, 87: 701–745.

Lamboy, M., 1994. Nannostructure and genesis of phosphorites from ODP Leg 112, the Peru margin. *Marine Geology*, 118: 5–22.

Laurin, J., 1996. *Sedimentary Discontinuities with Evidences of Phosphatic Mineralization as a Record of the Changes of Sea Level; Bohemian Cretaceous Basin.* M.Sc. Diploma thesis, Charles University, Prague, 122 pp. [In Czech, with English summary.]

Lepland, A., Joosu, L., Kirsimäe, K., Prave, A. R., Romashkin, A. E., Črne, A. E., Martin, A. P., Fallick, A. E., Somelar, P., Üpraus, K., Mänd, K., Roberts, N. M. W., van Zuilen, M. A., Wirth, R. & Schreiber, A., 2013. Potential influence of sulphur bacteria on Palaeoproterozoic phosphogenesis. *Nature Geoscience*, 7: 20–24.

Li, Y. & Schieber, J., 2015. On the origin of phosphate enriched interval in Chattanooga Shale (Upper Devonian) of Tennessee-A combined sedimentologic, petrographic and geochemical study. *Sedimentary Geology*, 329: 40–61.

Nathan, Y., Bremner, J. M., Loewenthal, R. E. & Monterio, P., 1993. Role of bacteria in phosphorite genesis. *Geomicrobiology*, 11: 69–76.

Palinska, K. A., Thomasius, C. F., Marquardt, J. & Golubic, S., 2006. Polygenetic evolution of cyanobacteria preserved as historic herbarium exsiccate. *International Journal of Systematic and Evolutionary Microbiology*, 58: 2253–2263.

Perdikatsis, B., 1991. X-ray powder diffraction study of francolite by the Rietveld method. Material Science Forum, 79/82: 809–814.

Philp, R. P. & Calvin, M., 1976. Possible origin for insoluble organic (kerogen) debris in sediments from insoluble cell wall materials of algae and bacteria. *Nature*, 262: 134–136.

Raff, E. C., Schollaert, K. L., Nelson, D. E, Donoghue, P. C., Thomas, C., Turner, F. R., Stein, B. D., Dong, X., Bengtson, S. & Huldtgren, T., 2008. Embryo fossilization is a biological process mediated by microbial biofilms. *Proceedings of the National Academy of Science, U.S.A.*, 105: 19360–19365.

Reimers, C. E., Kastner, M. & Garrison, R. E., 1990. The role of bacterial mats in phosphate mineralization with particular reference to Monterey Formation. In: Burnett, W. C. & Riggs, S. R. (eds), *Phosphate Deposits of the World* 3, Cambridge University Press, New York. pp. 300–311.

Regnier, P., Lasaga, A. C. & Berner, R. A., 1994. Mechanism of CO_3^{2-} substitution in carbonate-fluorapatite: Evidence from FTIR spectroscopy, ^{13}C NMR and quantum mechanical calculations. *American Mineralogist, 79*: 809–818.

Schieber, J., 1989. Pyrite mineralization in microbial mats from the mid-Proterozoic Newland Formation, Belt Supergroup, Montana, U.S.A. *Sedimentary Geology, 64*: 79–90.

She, Z.-B., Strother, P. & Papineau, D., 2014. Terminal Proterozoic cyanobacterial blooms and phosphogenesis documented by the Doushantuo granular phosphorites II: Microbial diversity and C isotopes. *Precambrian Research, 251*: 62–79

Schopf, J. W., Kudryavtsev, A. B., Czaja, A. D. & Tripathi, A. B., 2007. Evidence of Archean life: Stromatolites and microfossils. *Precambrian Research, 158*: 141–155.

Schulz, H. H., Jorgensen, B. B., Fossing, H. A. & Ramsing, N. B., 1996. Community structure of filamentous, sheath-building sulfur bacteria, *Thioploca* spp., off the coast of Chile. *Applied Environmental Microbiology, 62*: 1855–1862.

Schulz, H. N. & Schulz, H. D., 2005. Large sulfur bacteria and the formation of phosphorite. *Science, 307*: 416–418.

Schulz, H. N., Brinkhoff, T. Ferdelman, T. G., Hernández Mariné, M., Teske, A. & Jørgensen, B. B., 1999. Dense population of a giant sulfur bacterium in Namibian shelf sediments. *Science, 284*: 493–495.

Soudry, D. & Champetier, Y., 1983. Microbial processes in the Negev phosphorites (southern Israel). *Sedimentology, 30*: 411–423.

Soudry, D. & Lewy, Z., 1988. Microbially influenced formation of phosphate nodules and megafossil moulds (Negev, southern Israel). *Palaeogeography, Palaeoclimatology, Palaeoecology, 64*: 15–34.

Uličný, D., 1997. Sedimentation in a reactivated intra-continental strike-slip fault zone: The Bohemian Cretaceous Basin, Central Europe. In: *Abstracts, 18th IAS Regional European Meeting, Heidelberg. Gaea Heidelbergensis*, 3: 347.

Uličný, D., 2001. Depositional systems and sequence stratigraphy of coarse-grained deltas in a shallow-marine, strike-slip setting: the Bohemian Basin, Czech Republic. *Sedimentology, 48*: 599–628.

Uličný, D., Hladíková, J., Attrep Jr., M. J., Čech, S., Hradecká, L. & Svobodová, M., 1997. Sea-level changes and geochemical anomalies across the Cenomanian-Turonian boundary: Pecínov quarry, Bohemia. *Palaeogeography, Palaeoclimatology, Palaeoecology, 132*: 265–285.

Uličný, D., Špičáková, L., Grygar, R., Svobodová, M., Čech, S. and Laurin, J., 2009. Palaeodrainage systems at the basal unconformity of the Bohemian Cretaceous Basin: roles of inherited fault systems and basement lithology during the onset of basin filling. *Bulletin of Geosciences* 84, 577–610.

Valečka, J. & Skoček, V., 1991. Late Cretaceous lithoevents in the Bohemian Cretaceous Basin, Czechoslovakia. *Cretaceous Research, 12*: 561–577.

Vincent, W. F., 2009. Cyanobacteria. In: Likens, G. E. (ed.), *Encyclopedia of Inland Waters, vol. 3*. Elsevier, Oxford, pp. 226–232.

Vodrážka, R., Sklenář, J., Čech, S., Laurin, J. & Hradecká, L., 2009. Phosphatic intraclasts in shallow-water hemipelagic strata: a source of palaeoecological, taphonomic and biostratigraphic data (Upper Turonian, Bohemian Cretaceous Basin). *Cretaceous Research, 30*: 204–222.

Westall, F., 1999. The nature of fossil bacteria: a guide to the search for extraterrestrial life. *Journal of Geophysical Research, 104*: 16437–16451.

Whitney, D. L. and Evans, B. W., 2010. Abbreviations for names of rock-forming minerals. *American Mineralogist*, 95: 185–187.

Wiese, F., Čech, S., Ekrt, B., Košťák, M., Mazuch, M. & Voigt, S., 2004. The Upper Turonian of the Bohemian Cretaceous Basin (Czech Republic) exemplified by the Úpohlavy working quarry: integrated stratigraphy and palaeoceanography of a gateway to the Tethys. *Cretaceous Research, 25*: 329–352.

Williams, L. A. & Reimers, C., 1983. Role of bacterial mats in oxygen-deficient marine basins and coastal upwelling regions: Preliminary report. *Geology, 11*: 267–269.

Žítt, J., Nekvasilová, O., Hradecká, L., Svobodová, M. & Záruba, B., 1998. Rocky coast facies of the Unhost-Tursko High (Late Cenomanian-Turonian, Bohemian Cretaceous Basin). *Acta Musei Nationalis Pragae, Series B, Historia Naturalis, 54*: 79–116.

Žítt, J., Vodrážka, R., Hradecká, L., Svobodová, M., Šťastný, M. & Švábenická, L., 2015. Depositional and palaeoenvironmental variation of Lower Turonian nearshore facies in the Bohemian Cretaceous Basin, Czech Republic. *Cretaceous Research, 56*: 293–315.